Pitting on Carbon Cathodes in Aluminium Electrolysis Cells

Samuel Senanu[1], Tor Grande[2] and Arne Petter Ratvik[3]
1. PhD candidate
2. Professor
Department of Material Science and Engineering, NTNU Norwegian University of Science and Technology, NO-7491 Trondheim, Norway
3. Senior Research Scientist, SINTEF Industry, NO-7465 Trondheim, Norway
Corresponding author: samuel.senanu@ntnu.no

Abstract

Uneven cathode wear is one of the key challenges for the lifetime of aluminium electrolysis cells. Here we report on autopsy of several potlinings with focus on the surface morphology of the carbon cathodes. The surface morphology of the spent potlinings was characterized by measuring the profile by a laser interferometer, X-ray computed tomography and microscopy. The surface pitting of the cathodes resembles wide shallow pitting corrosion of metals. The characteristic size of the pittings is determined and compared to the size of the large aggregates constituting the cathode materials. No correlation between the characteristic size of the pitting and the aggregate size is observed. Based on the present findings, aggregate detachment is ruled out as a contributing mechanism to cathode wear.

Keywords: Pitting, cathode wear, carbon cathode, aluminium.

1. Introduction

Investigations of spent potlinings in aluminium electrolysis cells have shown a high degree of pitting in regions with potholes or significant cathode wear [1, 2]. Taberaux et al. [3] have reported that the maximum cathode wear was located under the anodes near the ends of the cathode blocks. They also reported that a pitted wear patterns at the locations with maximum cathode resembling pitting corrosion. Pitting on carbon cathodes has been suggested to arise from particulate detachment or subsurface processes [4]. The mechanism of pitting by particulate detachment or particle popping was also referred to by Siew et al. as a possible pothole initiation mechanism [5]. Pitting by particle detachment assumes a weakening of the binder due to preferred aluminium carbide formation within the binder, which results from the differences in the carbon structure of the aggregate and binder phase. The weakened binder results in the aggregate particles detaching from the carbon matrix leaving voids (pittings) that could initiate pothole formation [4, 5].

Pothole formation on cathodes that may be initiated by pitting, plays a very important role for the cathode life. A single pothole that reaches the current collector bar can result in a fatal failure of the pot by the molten metal dissolving the current collector bar resulting in a tap-out. Pothole formation is considered one of the predominant failure mode of some smelters in the aluminium industry [5, 6]. Here, we present a study of the pitting mechanism on carbon cathodes based on autopsy of spent potlinings from two different smelters. The cathodes are characterized by a combination of 3D scanning, optical microscopy and X-ray computed tomography.

2. Experimental

2.1. Autopsy and Sample Collection

Autopsies of five spent potlinings were performed in the study as summarized in Table 1. Prior to autopsy, all the pots were allowed to cool over a couple of days in a dry and enclosed space. After the spent potlining had cooled, bath and metal were carefully removed and finally vacuum cleaned to reveal all important details of the cathode surface. For easy documentation, the cathode blocks were numbered with a yellow marker.

Table 1. Summary of spent potlinings autopsied.

Pot	Arrangement/ Technology	Amperage(kA)/ Cathode Current density(A/cm²)	Pot age (days)	Carbon Cathode Type	Wear Pattern	Comments
1	Side by Side Prebake	313 / 0.8	2461	Graphitized and Impregnated	WW	Planned shutdown
2	End to End Prebake	175 / 0.8	1028	Graphitic (100% Graphite aggregate)	W	Tapout
3	End to End Prebake	175 / 0.8	3154	Graphitic (100% Graphite aggregate)	W	Planned shutdown
4	End to End Prebake	175 / 0.8	2849	Graphitic (100% Graphite aggregate)	W	Planned shutdown
5	Side by Side Prebake	313 / 0.8	1731	Graphitized and High Density	WW	Tapout

Locations with important information such as pitting, potholes, sludge, crack, metal plugs, etc. were first photographed before analysis commenced. After photography, wear patterns or profiles were measured employing laser interferometer (3D Freestyle scanner) and manual measurement. Figure 1 is a picture of a section of a cleaned spent potlining ready for autopsy analysis.

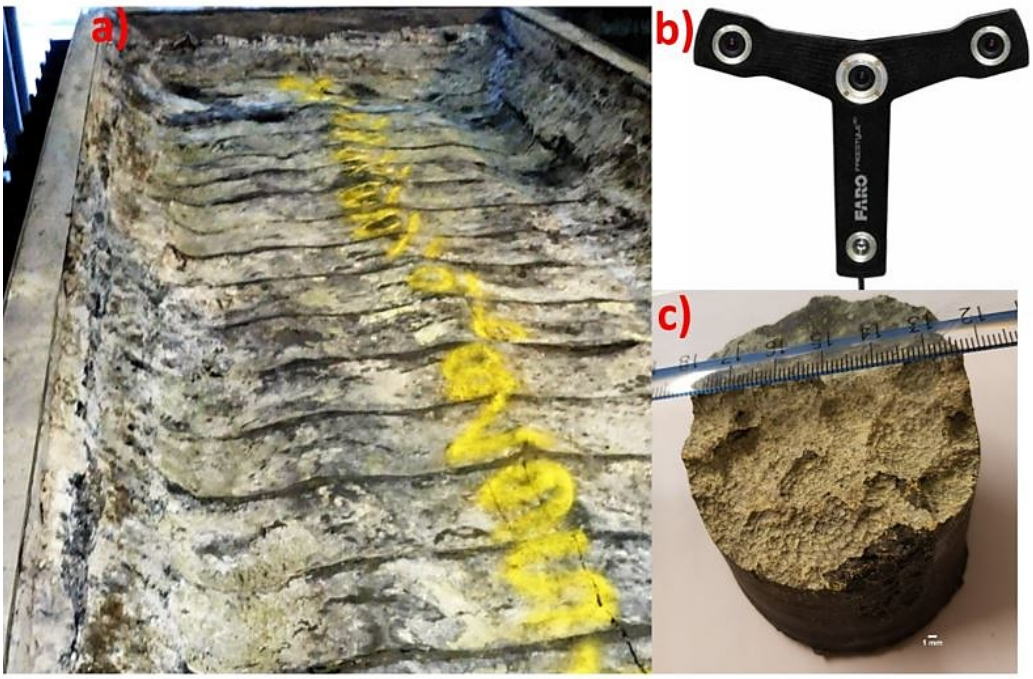

Figure 1. Autopsy of spent potlining. a) Image of the cathode surface after vacuum cleaning. b) Freestyle Handheld 3D scanner for surface profile measurements. c) Autopsy sample drilled from the spent potlining for analysis.

2.2. Characterization of the Autopsy Samples

The autopsy samples collected were analysed using X-ray computed tomography (CT scanning). No prior preparation was done for the samples to be analysed. A Nikon XTH225ST instrument (cone beam volume CT) was employed for the CT data acquisition. For the analysis, a tungsten reflection target was used together with an acceleration voltage of 140 kV and a current of 135 µA. Imaging

was done using an integration time of 1 second, amplification of 18 dB and 3142 projections per 360°. The sample was placed 226.7 mm from the source and the detector was kept at 1124.8 mm from the source. Detector size applied was 400x400 mm, resulting in a voxel size of 40.2 µm. The images were exported as 16-bit TIFF and processed using ImageJ software. Linear intercept method was employed to determine the average grain size of the carbon aggregates. The method involved drawing at least 20 parallel lines (parallel to x or y-axis) of known length through the CT images obtained from the CT scanning. The average grain size was obtained by the intercept method by finding the average of all the values obtained by dividing the length of each parallel line by the number of grains intercepted by it.

For the microstructural analysis, the samples were cut into smaller samples, imbedded into epoxy or current conducting polyfax and mechanically polished to obtain smooth surfaces. Optical microscopy was performed using the REICHERT MeF3A optical microscope. A FARO freestyle handheld 3D scanner was used to acquire 3D data of the whole cathode surface of pot 5. The acquired data were used to construct 3D images of the surface profile of the spent potlining. From these 3D images the pitting at the upstream and downstream ends of the cathode blocks were characterized. MeshLab software program was used for analysing the 3D data.

3. Results

3.1. Visual Observations

Visual observation of all the five spent potlinings showed trends similar to observations reported from previous autopsies [2, 3, 7, 8]. The maximum wear was located at the ends of the cathode blocks and characterized by pitting (pitted wear). Pitting was observed for all the carbon cathode types (graphitic and graphitized) investigated. Figure 2 is a 3D image of a section of the spent potlining obtained from analysing the scanning data from pot 5. From the 3D image, the count density and size distribution of pitting within a chosen area of the cathode block was obtained from which a histogram was plotted. The histogram for pitting on the upstream and downstream ends of two of the cathode blocks is shown in Figure 3. The histogram shows that the downstream ends of the two cathode blocks have a relatively lower count density of pitting than the upstream ends.

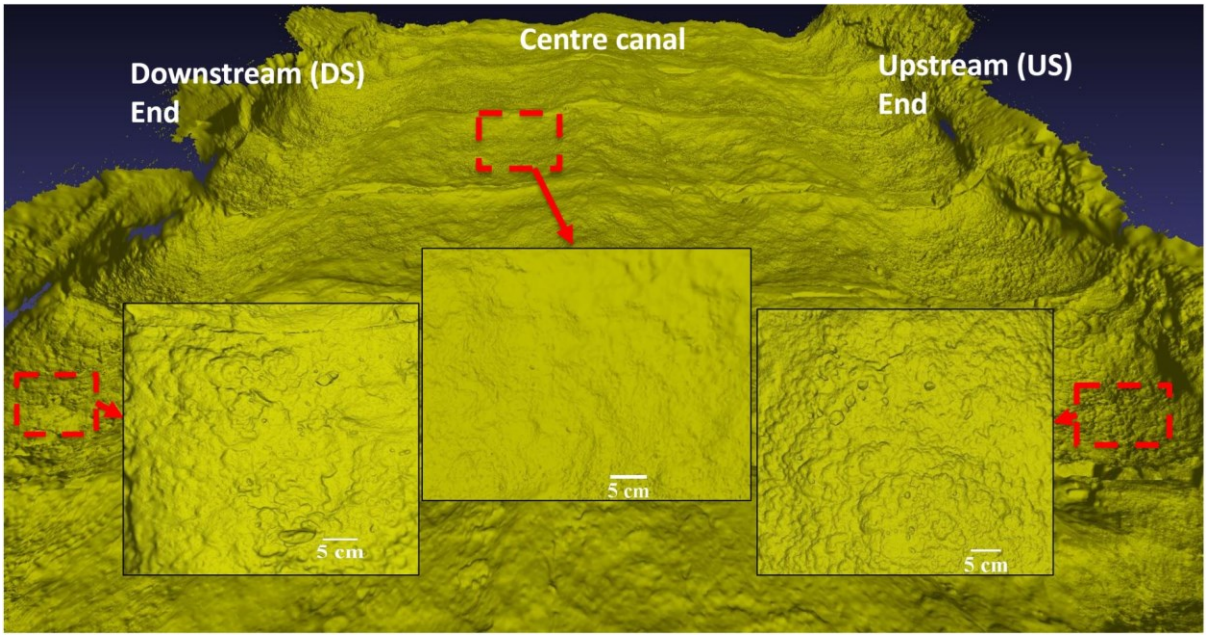

Figure 2. 3D image of a spent potlining showing the occurrence of pitting at the centre canal as well as the upstream and downstream ends of a graphitized cathode block (pot 5).

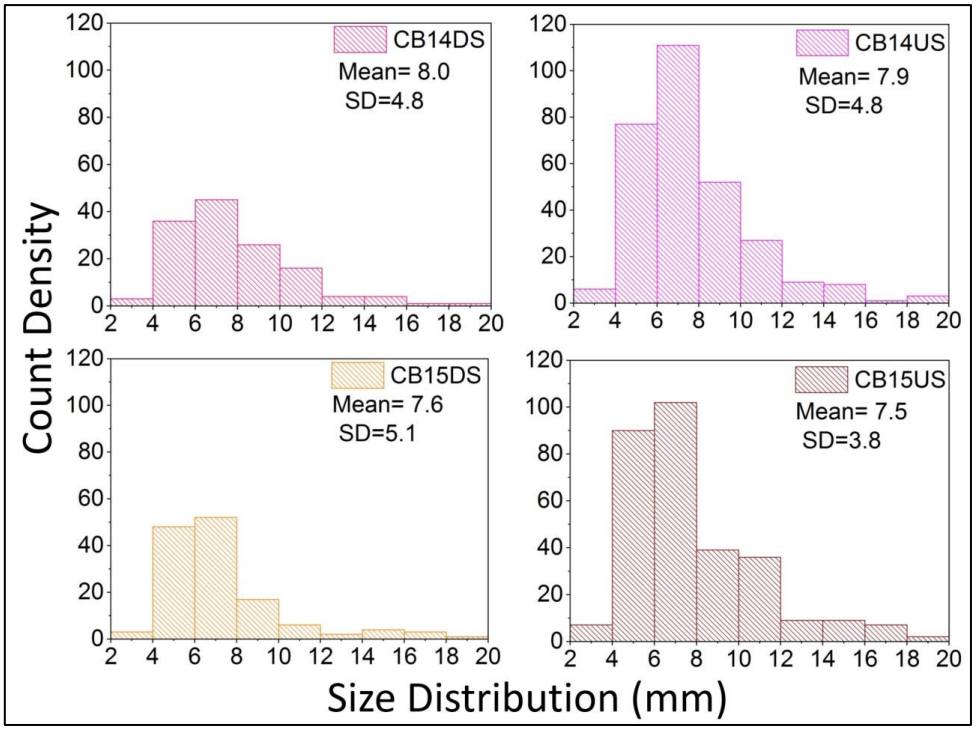

Figure 3. Histogram showing the count density and size distribution of pitting on the upstream and downstream ends of 2 carbon cathode blocks (cathode blocks 14 and 15) from pot 5.

Generally, it was observed that for the graphitic cathode blocks, pitting was present all over the cathode surface. There were, however, differences in the size of the pitting on these graphitic cathode blocks. The pitting closest to the ends of the cathode blocks where the wear was highest, had a relatively larger diameter than the ones closest to the centre canal, Figure 4 illustrates this. For the graphitized cathode blocks, pitting was present mostly at the ends of the cathode blocks where the wear was most pronounced, no distinct pitting was observed at the central canal. This observation is well illustrated by Figure 2.

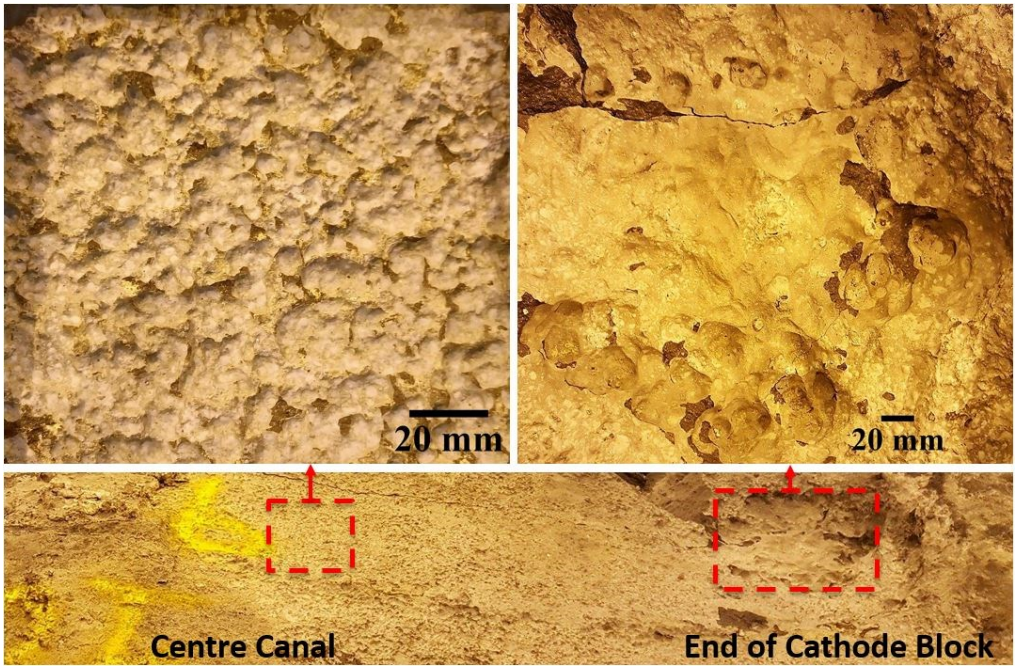

Figure 4. Photograph of a spent potlining with graphitic cathode block (pot 6057) showing pitting all over the surface. Highlighted images show the differences in pitting sizes between the centre and side of the cathode block.

Pitting was also observed on the ramming joints between the cathode blocks at the locations with highest degree of pitting as shown in Figure 5. One of the spent potlinings (pot 5) that was investigated had a tapout through a pothole on one of the carbon blocks. A closer investigation of the location surrounding the pothole revealed a very high degree of pitting. Figure 6 is a picture showing the tapout hole in the cathode block.

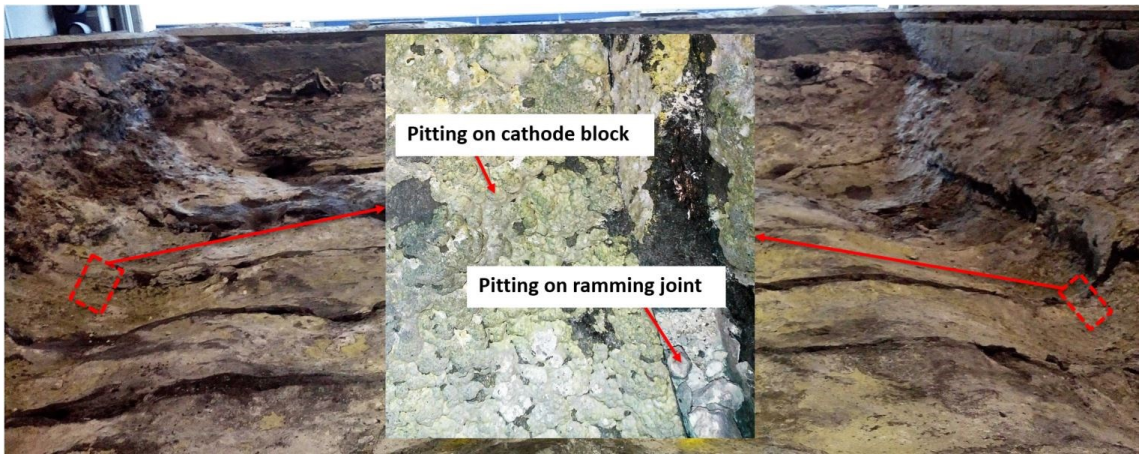

Figure 5. Photograph of a section of a spent potlining with a graphitized cathode block (pot 1) showing pitting mostly at ends of cathode block. The insert image shows the pitting mainly observed at the ends of the cathode blocks and ramming joints.

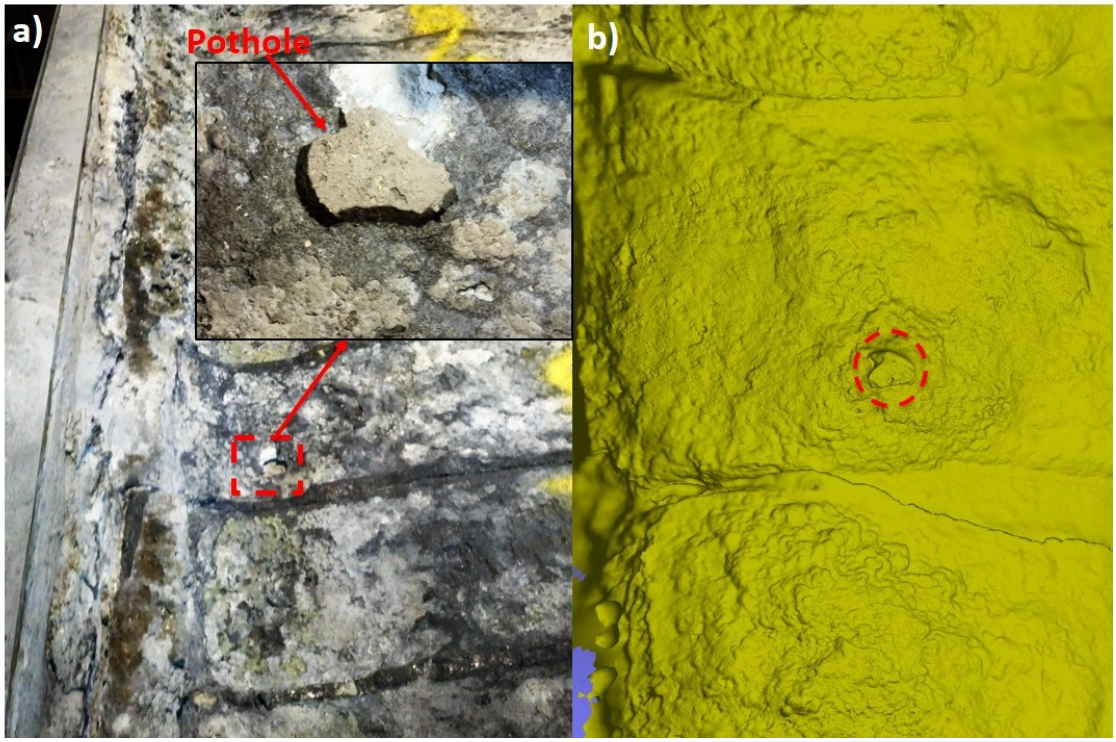

Figure 6. Pothole formation on carbon cathode blocks from pot 5. a) Section showing location of tapout on carbon cathode. b) A 3D image of the tapout location in the pothole on the carbon cathode.

3.2. Laboratory Analysis

The different phases, porosity and topography of the autopsy samples were obtained by computed tomography (CT) images. The phases and pores were observed as different shades of grey. Bath components are identified as white areas while the carbon materials can be seen as different scales of

grey, where the coarse aggregates are dark grey and the binder phase with the fine aggregate is light grey. The contrast between the different carbon components allowed for determining the average size of the coarse aggregates using the linear intercept method. Figure 7 shows CT images of four of the cathode samples collected from pot 5. The average coarse grain size was determined by the linear intercept method to be 3.2 mm.

In addition to determining the grain size, the CT images were also used to analyse the topography of the eroded surface of the samples. This was done by three-dimensional investigation of the CT images. A closer investigation of these images revealed that part of aggregates are still within the carbon matrix and partly eroded aggregates were present at the surface. This was observed for all the 5 cathode samples analysed. Figure 8 shows CT images of one of the 5 samples analysed showing remains of aggregates within the carbon matrix.

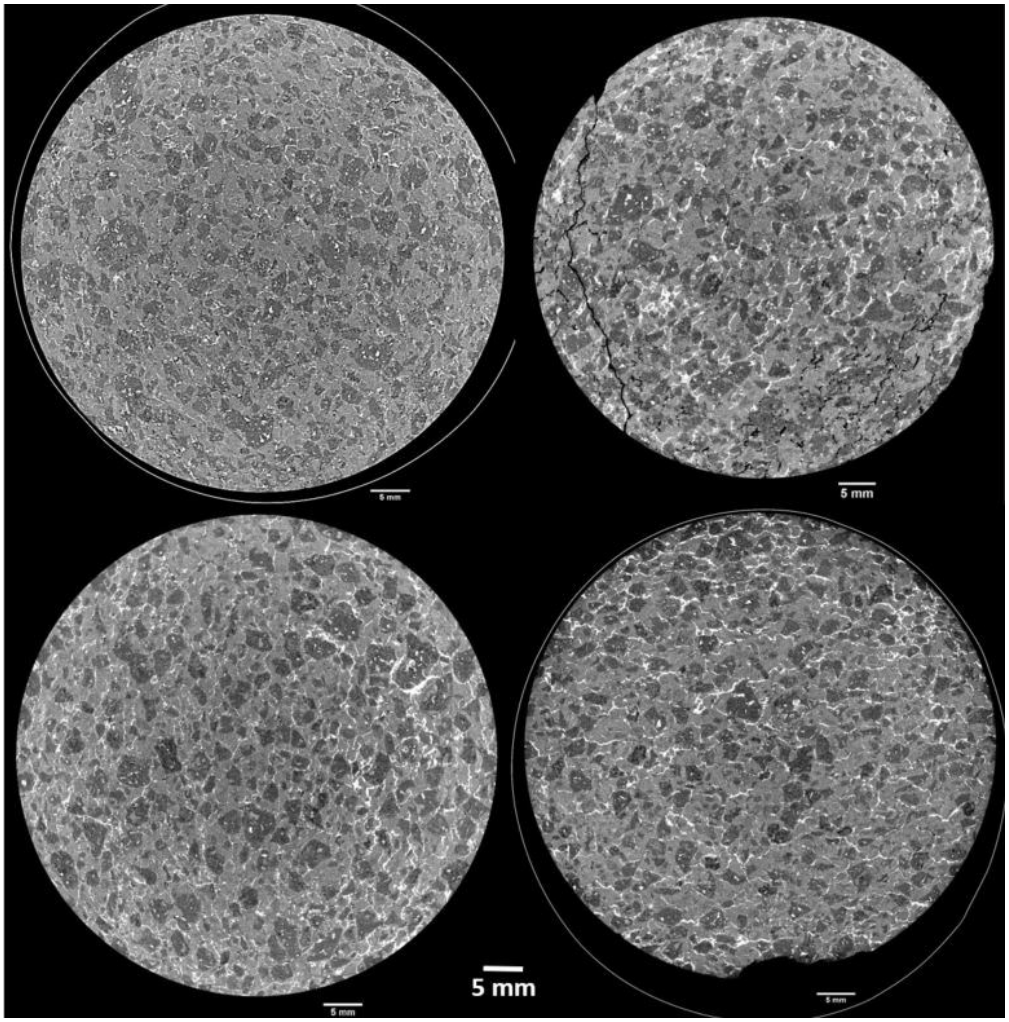

Figure 7. CT images of the cross-section of the autopsy samples used for the linear intercept method to determine the average grain size of carbon aggregates.

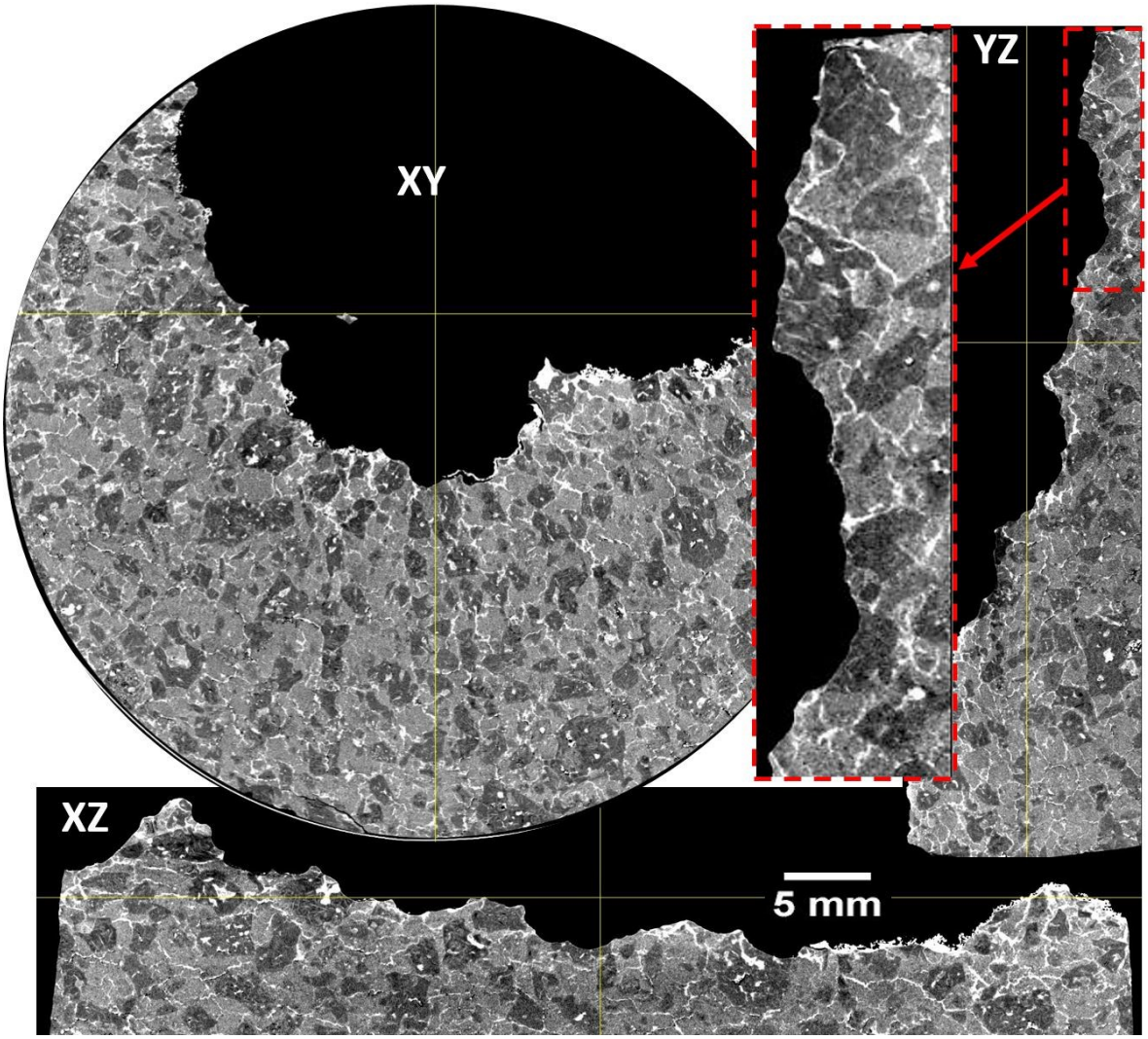

Figure 8. CT image of a cathode sample with pitting. Closer analysis of the XZ and YZ cross-sections show remains of aggregate grains within the carbon cathode matrix as illustrated by the highlighted section of YZ direction image.

Optical microscopy was also employed to further investigate the interface between the carbon and bath/carbide, specifically at locations with pitting. The interface of all the cathode types (graphitic and graphitized) were evaluated using this technique. It was observed for all the cathode types that remains of the aggregate was left within the carbon matrix. A relatively even eroded carbon interface was observed for all the cathode types. Figure 9 show optical micrographs representative of all the cathode types investigated during the autopsies.

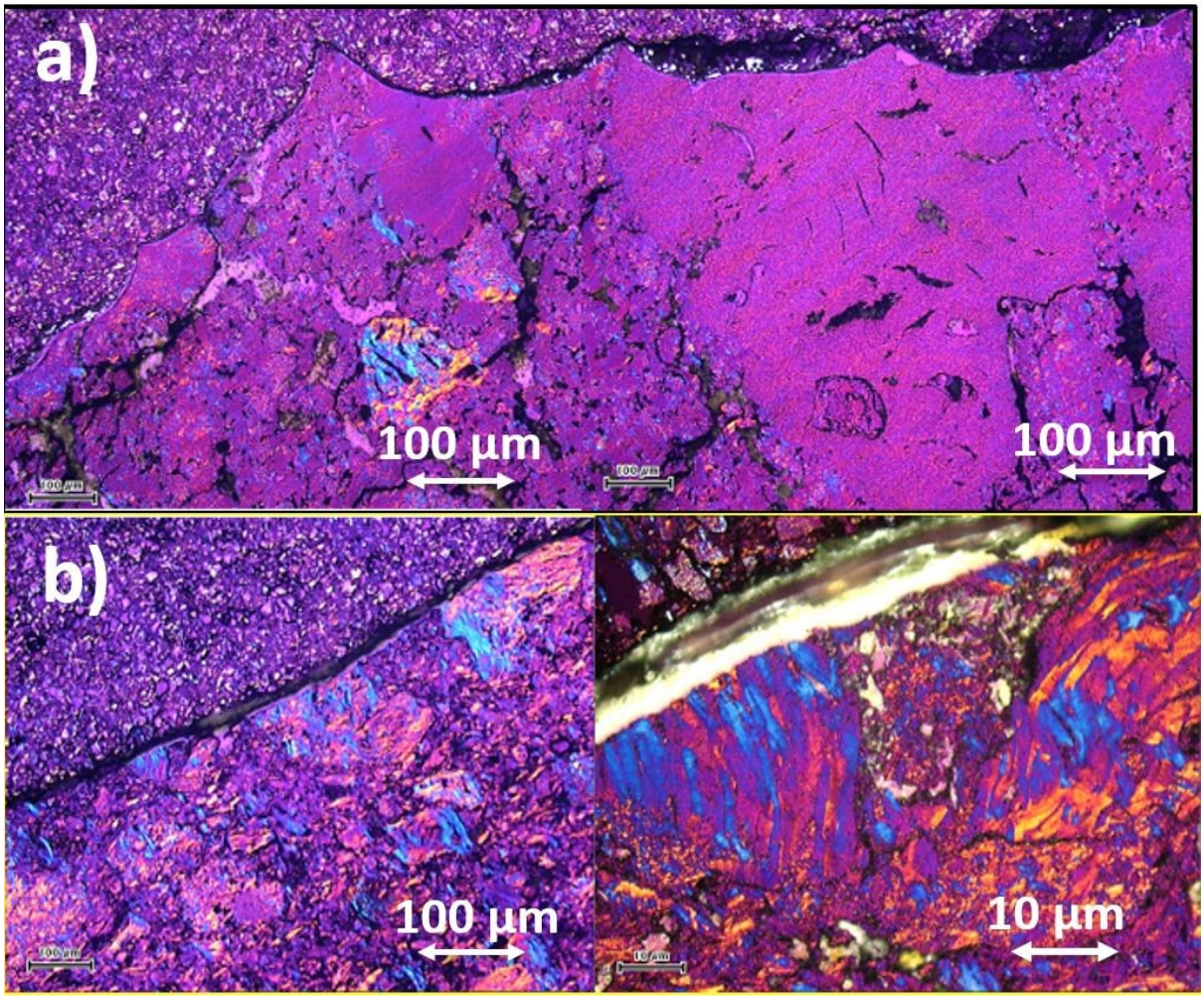

Figure 9. Optical micrographs of the interface between carbon and bath for the autopsy sample analysis. a) High-density Graphitized cathode block from pot 5. b) Graphitic cathode block from pot 3.

4. Discussion

4.1. Cathode Wear by Pitting

Figure 6 shows a pothole that resulted in a tapout of a cell after just 1731 days. The pothole occurred at the upstream end of the cathode block of a spent potlining (pot 5) investigated during the autopsy. Examination, as well as wear measurements by other autopsies, show that the wear is highest at these locations (cathode block ends) [2, 3, 6, 7]. It has also been reported that the wear in these locations is pitted [2, 3], suggesting pitting as a wear mechanism in these locations as shown in Figure 10. A closer look at the 3D image (Figure 6) obtained from the location with the pothole that led to the tapout shows that pitting might have been a precursor to the pothole formation.

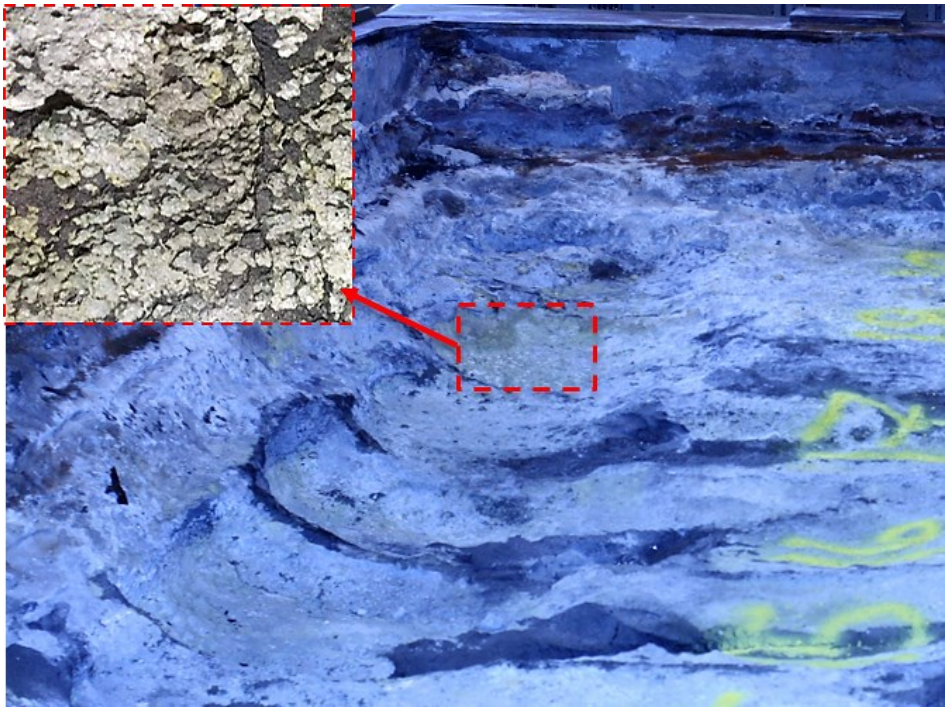

Figure 10. Pitting on the surface of a spent potlining (pot 1). The highlighted area shows the high degree of pitting that characterizes locations with maximum wear.

4.2. Pitting Mechanisms

Pitting on carbon cathodes have been suggested to occur as a result of particle detachment or pure electrochemical corrosion. [2, 9]. The pitting mechanism by the particle detachment is illustrated in Figure 11. This hypothesis is based on the fact that the porous nature of the carbon materials allows for bath penetration into the binder carbon material. This increases the probability for formation of aluminium carbide within the carbon material, particularly in the more amorphous binder matrix resulting in weakening of the carbon material. Particle or aggregate detachment resulting from dissolution of the binder matrix holding them together will then occur and the voids created are observed as pitting on the carbon cathode [9].

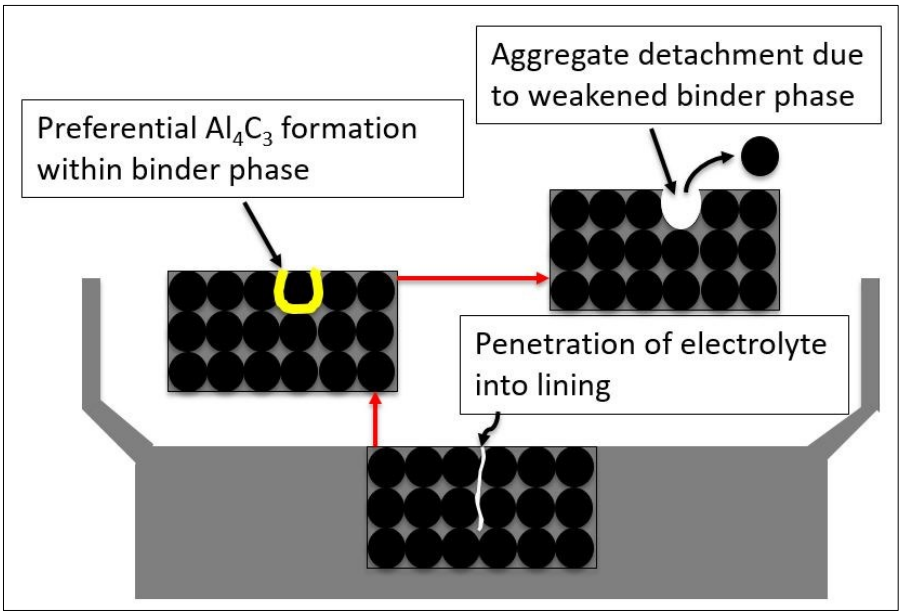

Figure 11. Mechanism of pitting by particle detachment due to the weakening of binder phase [5, 9].

All the autopsies conducted demonstrate the presence of pitting on the carbon cathode surface irrespective of the type of carbon material or grade of the carbon cathode block. Figure 5 is a picture showing pitting on both the cathode block and ramming joints. This suggests that pitting is essential for the carbon cathode wear mechanism. There is, however, a difference in the amount of pitting observed on the graphitized and graphitic cathode blocks. While the graphitized cathode blocks showed distinct pitting mainly at the ends of the cathode blocks, the graphitic cathode blocks show pitting almost all over the carbon cathode surface. The images in Figures 2 and 4 show these differences. The appearance of pitting all over the graphitic cathode blocks is assumed to be due to their relatively high porous nature as compared to the graphitized cathodes, resulting in a relatively higher electrical resistivity that contributes to a more even current distribution over the cathode.

The varying sizes of the pitting on the graphitic cathode blocks with respect to the centre canal and the ends of the cathode blocks as shown by Figure 4 may be explained by the combination of high current densities and faster transport rates. The high current densities at the ends of the cathode block will lead to an increase in the electrochemical formation of aluminium carbide. The high current densities will also induce high electromagnetic movements in the metal and bath leading to an increase in the dissolution and transport of aluminium carbide at the cathode block ends as compared to the centre canals [6, 10]. For the graphitized cathode blocks, the high degree of pitting at the ends as compared to the centre with almost no pittings may also be because of the high current density and the induced high movements in metal and bath and thus higher dissolution and transport of aluminium carbide.

In order to verify the particle detachment mechanism, the average grain sizes of the carbon aggregates and the average sizes of the pittings were determined. Figure 3 shows the size distribution of the pittings observed from the autopsy of pot 5. The average grain sizes of the carbon aggregates were also determined by analysing the CT images of the autopsy samples as shown in Figure 7 using the linear intercept methods. Comparing the average sizes of pittings to the average grain sizes of the carbon aggregates did not yield any correlation. This observation does not support grain detachments as the main mechanism for the observed pitting.

Investigation of CT images obtained from the CT analysis of the autopsy samples as illustrated in Figure 8 show remains of the carbon aggregates within the pittings. This would not be the case if particle detachment was the main mechanism for the pitting as the whole grain would have detached out of the matrix. This observation of aggregate remains within carbon matrix was further confirmed by the optical microscope images of the same autopsy samples as shown in Figure 9. Finally, the relatively uniform wear surface within these pittings, as shown by the optical micrographs (Figure 9), suggests that the pittings observed on the carbon cathodes might have formed by a chemical or electrochemical corrosion process other than a physical or mechanical detachment process.

5. Conclusions

Pitting on carbon cathodes are observed in all the autopsies carried out in this work. This is particularly the case at the locations with the highest wear, such as the ends of the cathode blocks. The observation that graphitic cathode blocks show pitting almost all over the cathode surface including the centre canal while graphitized cathode blocks only show distinct pitting at the cathode block ends may suggest a more even current density distribution for the graphitic blocks owing to their more porous nature and high electrical resistivity. The fact that pitting becomes more pronounced at the ends of the cathode blocks (graphitic and graphitized) may suggest, current density, carbide dissolution and transport rates play a role in their formation and development.

Non-correlation between the average pitting sizes and average grain sizes in addition to remains of aggregates within the carbon matrix at locations with pittings suggest that particle detachment is not the main cause of pitting on carbon cathodes. The mechanism for pitting is more likely to be chemical or electrochemical in nature.

6. Acknowledgements

Financial support from the Norwegian Research Council and the partners Hydro, Alcoa, Elkem Carbon and Skamol through the project "Reactivity of Carbon and Refractory Materials used in Metal Production Technology" (CaRMa) is acknowledged.

7. References

1. Samuel Senanu, Tor Grande, and Arne Petter Ratvik, Role of pitting in the formation of potholes on carbon cathodes- a review, *in Proceedings of 34th International ICSOBA Conference*, Quebec, Canada, 3 - 6 October 2016, Paper AL31, *Travaux* 45, 787-796.
2. Samuel Senanu et al., Cathode wear based on autopsy of a shutdown aluminium electrolysis cell. *Light Metals 2017*, 561-570.
3. Alton T. Tabereaux et al., Erosion of cathode blocks in 180 ka prebake cells. *Light Metals 1999*, 187-192.
4. Parin Rafiei, et al., Electrolytic degradation within cathode materials. *Light Metals 2001*, 747-752.
5. Eng Fui Siew et al., A study of the fundamentals of pothole formation. *Light Metals 2005*, 763-769.
6. Morten Sørlie and Harald A. Øye, *Cathodes in aluminium electrolysis*. 3rd ed.: Aluminium-Verlag, Düsseldorf, 2010.
7. Pierre Reny and Siegfried Wilkening, Graphite cathode wear study at alouette. *Light Metals 2000*, 399-404.
8. Egil Skybakmoen, et al., Measurement of cathode surface wear profiles by laser scanning. *Light Metals 2011*, 1061-1066.
9. Pretesh Patel, Margaret Hyland, and Frank Hiltmann, Influence of internal cathode structure on behavior during electrolysis part ii: Porosity and wear mechanisms in graphitized cathode material. *Light Metals 2005*, 757-762.
10. Kristin Vasshaug, *The influence of the formation and dissolution of aluminium carbide on the cathode wear in aluminium electrolysis cells*, Norwegian University of Science and Technology, Trondheim, Norway, 2008.